STM JOURNALS

Journal of
Experimental & Applied Mechanics

https://journals.stmjournals.com/joeam

ISSN: 2230-9845 (Online)
ISSN: 2321-516X (Print)
Volume 17, Issue 1, 2026
January–April
DOI (Journal): 10.37591/JoEAM

Research JoEAM

Effect of Thermal Conditions on Microstructure and Mechanical Properties of AA5083 Processed by Equal Channel Angular Pressing

Nagendra Singh[1,*], Sanjeev Kumar Verma[2]

Abstract

A commercial AA5083 with an initial grain size of 210 μm was given an ultrafine-grained structure using the equal channel angular pressing (ECAP) technique under die design as patented. The identical sample underwent two successful passes through the die at 473 K, with each passage causing the sample to rotate 90° along its own longitudinal axis. After just one pressing, the microstructure was comparatively homogeneous. It was made up of elongated substructure parallel bonds that were 0.9 μm in length and 0.3 μm in breadth on average. Two passes yielded an equiaxed super fine-grained structure of 0.4 μm in the current alloy. The minuscule granules maintained their thermal stability at 548 K. The yielding strength of the as received AA5083 was 132 MPa; however, after one pressing, it rose to 252 MPa, and after two passes, it reached 293 MPa, which was higher than the yield stress of a typical AA5083. The AA5083, with a 0.4 μm grain size, was found to exhibit superplastic-like behavior below 548 K, with an elongation to failure of almost 210%. Using ECAP at 498 K, AA5083 was treated in this study to yield an ultrafine particle size of roughly 210 nm.

Keywords: AA5083, ECAP, low-temperature superplasticity, tensile properties, UFG structure

INTRODUCTION

Several studies have recently attempted to apply severe plastic deformation to metallic materials to reduce the grain size to the sub-micrometer level. Using severe plastic deformation techniques, numerous bulk metallic materials have been successfully fabricated with a sub-micrometer, incredibly fine-grained structure, including accumulative roll bonding, equal channel angular pressing (ECAP), and severe torsional straining [1, 2]. The equal channel angular pressing (ECAP) method has been successfully applied to generate diverse bulk ultrafine-grain materials without residual porosity [3, 4]. Examples of these materials include Armco iron [3–4], Al alloys and their composites [5–9], Cu [10–13], Mg alloys [5], pure Ni [3], low-carbon steel [14–19], Ti alloys [20–22], and Zn-22%Al [23]. Aluminum alloys, in particular, have gained popularity as a lightweight, extremely effective material to address the issues of energy and environmental pollution in all industrial sectors. Owing to their excellent formability, weldability, resistance to corrosion, and high strength from solid solution and work hardening, Al–Mg system alloys are among the most extensively used Al alloys in wrought materials [24]. One benefit of ECAP is the possibility of achieving a sub-micron grain size. ECAP was performed with a path that involved up to two passes at 498 K, deforming AA5083. Deformation altered the grain size from approximately 210 μm to 310 nm. Approximately 825 K is a high-temperature area, and the specific heat capacity increases monotonically with increasing temperature. The current disclosure pertains to a process that uses ECAP to produce

***Author for Correspondence**
Nagendra Singh
E-mail: singh.mech2008@gmail.com

[1]Assistant Professor, Department of Mechanical Engineering, Institute of Engineering and Technology, Dr. Bhimrao Ambedkar University, Swami Vivekanada Campus, Khandari, Agra, Uttar Pradesh, India
[2]Assistant Professor Department of Mechanical Engineering, Central Instrumentation Facility, Research and Development Cell, Lovely Professional University, Phagwara, Punjab, India

Received Date: January 22, 2026
Accepted Date: February 01, 2026
Published Date: February 16, 2026

Citation: Nagendra Singh, Sanjeev Kumar Verma. Effect of Thermal Conditions on Microstructure and Mechanical Properties of AA5083 Processed by Equal Channel Angular Pressing. Journal of Experimental & Applied Mechanics. 2026; 17(1): 49–64p.

metal wire with improved electroconductivity and mechanical properties. Important developments in the field of severe plastic deformation technology are represented by patented die designs for ECAP [25]. To maximize the ECAP process, which is utilized to improve mechanical properties, refine microstructures, and raise the general quality of processed materials, these patents frequently contain novel advancements in die geometry, material, and function. Modifying channel angles, entry, and exit zones, and corner radii to create controlled shear strain and lessen frequent problems, such as stress concentrations and frictional resistance, are usually key components of patented ECAP die designs. Certain patents describe variable-angle or multi-channel dies, which save time and improve material homogeneity by enabling flexible processing of various materials or multi-pass processing without sample removal.

Superplastic Al–Mg system alloys have attracted considerable attention because they can achieve the high forming rates required for superplastic forming to maintain the present fabrication speed. The forming temperature should be as low as practicable to save fabrication energy and avoid cavities, grain formation, and solute loss from surface layers [26]. In metallic materials, the grain size has a significant impact on superplasticity. To achieve a fine-grained structure, thermomechanical treatment is typically employed in Al–Zn–Mg system alloys [27–31] and Al–Li system alloys [32]. Additionally, Horita et al. [33, 34] produced the highest strength among non-heat-treated type Al alloys with an average grain size of less than 1.2 μm in the commercial AA5083 by using ECAP under specific conditions [35–37]. Additionally, they investigated the tensile and thermal stability of ECAP AA5083 at room temperature. However, studies on the mechanical characteristics and microstructure of commercial AA5083 pressed under different conditions using the ECAP process are still lacking. Furthermore, investigations have been conducted on the low-temperature superplasticity of Al–Mg [33, 34, 38–40] or Al–Mg–Mn [40–43] alloys.

The low-temperature superplasticity of commercial AA5083 through ECAP has not been thoroughly examined. The objective of this study was to evaluate the viability of superplasticity at relatively low temperatures after obtaining an ultrafine-grained structure of commercial AA5083 by ECAP and to examine the microstructural and mechanical characteristics at room and elevated temperatures. Research on reducing the grain size to less than a sub-micron is currently being conducted to enhance the mechanical properties of materials, including superplasticity, as well as their toughness and strength. Some techniques have been used to miniaturize the grains of current materials; however, none of these techniques can reduce the grain size to less than a sub-micron, and they can only reduce the deformation caused by a decrease in cross-section as the processing quantity increases. Extreme plastic deformation is a technique used to solve such issues; it causes extreme plastic deformation within the material, which miniaturizes the grains of the material. ECAP produces transverse shear deformation by applying flexion to a die with similar channels, which rapidly miniaturizes bulk material grains [44, 45]. There are four processing steps involved in modifying the grain structure of a material [45]. Dislocations form and become entangled in the different slip systems during Stage 1 of work hardening, which increases the dislocation velocity. Stage 2 produces cells with a grain-like structure by creating a dislocation network and continuously increasing the dislocation velocity. The cell size decreases during this step as the processed quantity and dislocation velocity increases. In Stage 3, the subgrain is where a stable Low-Angle Grain Boundary (LAG). Boundary is formed by the dislocation interacting with a high-density dislocation to generate dynamic recovery. In Stage 4, ultrafine grains with an orientation difference of over 15° and an increase in dislocation velocity transform the LAG boundary into a high-angle grain boundary. Regardless of the number of processing steps, materials treated with ECAP are likely to see increases in strength and toughness without losing sectional area or experiencing air space. This is a method that, by accelerating the creation of a high-angle grain boundary, can achieve low-temperature superplasticity. It is a helpful approach for measuring many different parameters, such as the energy of activation, glass transition temperature, recrystallization temperature, latent heat, and specific heat. The behavior of the precipitates from supersaturated magnesium is beneficial for Al–Mg alloys [46, 47].

AA5083, a commonly used non-heat-treated Al–Mg alloy, is inexpensive, strong, oxidation-resistant, highly formable, and has low density. Consequently, it can reduce energy consumption by making car planks and vessels lighter than they currently are because all studies to date have focused exclusively on the mechanical characteristics of the commercial AA5083 produced by ECAP [48, 49]. Using a specific heat capacity, a common feature of the physical characteristics of materials treated by ECAP, we measured the energy accumulation inside the grain formation structure.

EXPERIMENTAL PROCEDURES

An extruded bar with the mass percentage composition of AA5083 is shown in Table 1. The pre-materials for the ECAP were annealed samples. Pre-materials AA5083 had an average grain size of about 210 μm. MoS_2 was used as a lubricant, and ECAP was performed at 498 K with a press speed of 2.2 mm s^{-1}. The inner angle and arc of curvature of the present ECAPed die were 90° and 120°, respectively, at the external point of contact between the channels on the die. To produce an effective strain of 1 in a single pass [44, 45]. The sample was rotated about its longitudinal axis between each pressing step of the ECAP technique.

This pressing pattern is referred to as the route. The route was selected because, with each different pressing option, it restores the segment to its initial shape, thereby enabling the creation of an almost equiaxed ultrafine grain structure [17, 18, 46]. An Instron machine was used to perform tensile testing on full-scale specimens with a gauge length of 28 mm at room temperature and an initial strain rate of 1.02×10^{-3} s^{-1}. Tensile specimens with an initial strain rate of 1.06×10^{-4} s^{-1} and a gauge length of 8 mm were subjected to tensile testing at 548 K. Vickers microhardness testers were used to measure the microhardness, whereas JEOL 2010 transmission electron microscopes operating at 210 keV were used to study the microhardness [47–52].

The extrudate was shaped into a circular bar specimen with a diameter of 10 mm and a length of 50 mm. Annealing for 1.2 h at 748 K produced grain samples with a diameter of 210 μm for the round bar specimen. The specimen surface was coated with MoS_2 lubricant to reduce friction with the die. A schematic representation of the ECAP pressing die is shown in Figure 1. The sample was removed from the die and pressed once more in Route *A* without rotation. The sample was rotated through 90° the Route B_c between each pressing. Route repeated pressings, from one to two pressings through the die, were carried out on distinct samples under both *A* and B_c conditions [53]. The results of a previous study [54] indicate that when ψ is 90°, the maximum strain can be achieved with a single pressing.

The effective strain (ϵ) that the specimen accumulates during the ECAP process can be broadly represented by the following equation.

$$\varepsilon = N\left[\frac{2\cot[\phi/2+\psi/2]+\psi\operatorname{cosec}[\phi/2+\psi/2]}{\sqrt{3}}\right] \quad (1)$$

Here, *N* indicates the number of times the specimen was run through the die process. Equation (1) simplifies the determination of the strain quantity based on the die dimensions; regardless of $\psi = 90°$ the situation, one pass can yield the effective strain that is approximately 1. A specimen that weighs approximately 100 mg and has dimensions of 4 mm in diameter and 2.5 mm in thickness was used to measure the specific heat capacity [55]. Additionally, a 210 keV acceleration voltage and a JEOL 2010 transmission electron microscope (TEM) were utilized to observe the microstructure within the material. The specimen was jet-polished in a combined solution of 28% nitric acid and 72% methanol at a voltage of 28 V to observe it under a TEM. Additionally, diluted Poulton's reagent was used to prepare the material for optical examination.

Table 1. Aluminum alloy 5083 chemical composition.

Element	Si	Fe	Cu	Mn	Mg	Zn	Ti	Cr	Al
% Present	0.4	0.4	0.1	0.4-1.0	4.0-4.9	0.25	0.15	0.05-0.25	Balance

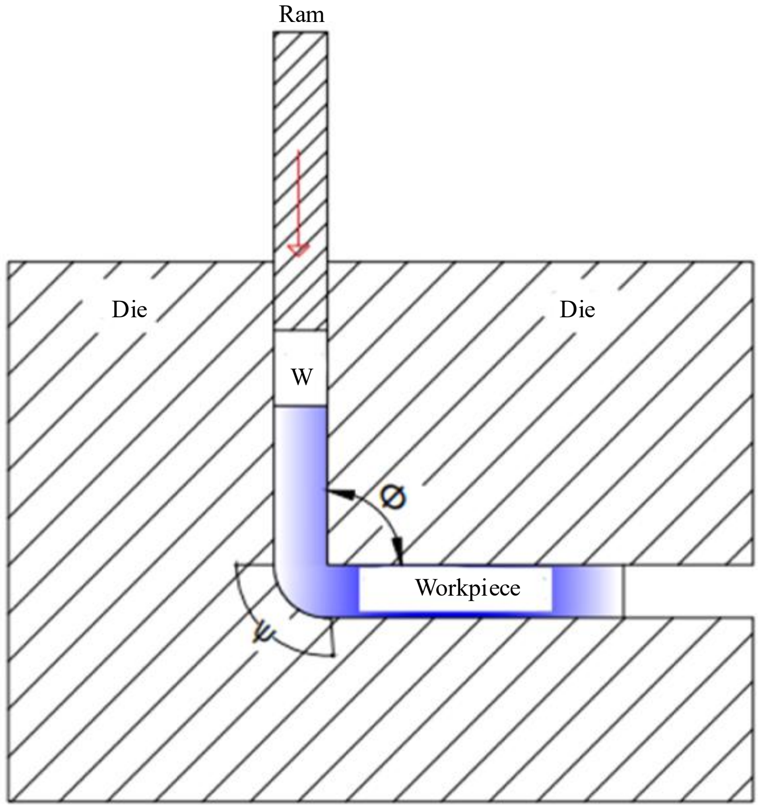

Figure 1. Schematic diagram of ECAPed die [11].

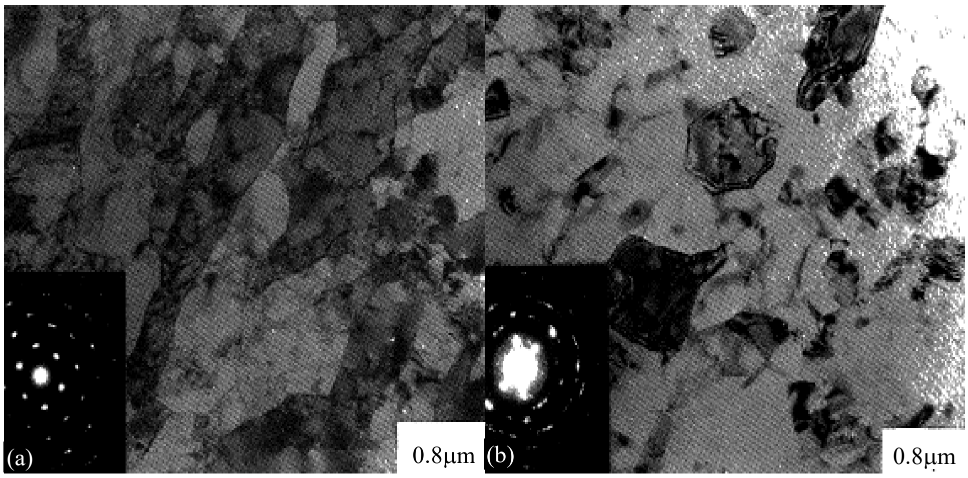

Figure 2. (a) to (b) ECAP-pressed AA5083's TEM microstructure and matching Selected Area Electron Diffraction. (SAED) patterns after (a) one pressing, and (b) two pressings [15].

RESULTS AND DISCUSSION

Microstructural Characterization of Materials

Microstructural Evolution During Equal Channel Angular Pressing

TEM micrographs of equal channel angular pressing (AA5083) with the number of pressings are shown in Figure 2. The microstructure resulting from single pressing consisted mostly of parallel bands of elongated grains, each with a length of 0.9 μm and a width of 0.3 μm. Relatively clear patches characterized the associated SAED patterns. This suggests that low-angled borders would be present in the majority of fine-grain boundaries created by single pressing. After undergoing two pressing routes, the microstructure exhibited predominantly equiaxed fine grains, and the subgrain band alignment with the shear direction disappeared. The establishment of a high-angle boundary was indicated by the appearance of additional and diffused dots in the SAED pattern. One and two pressings produced nearly equiaxed extremely fine grains, approximately 0.4 μm in size. Furthermore, in comparison to earlier patterns, the SAED pattern had more rings and more evenly distributed dots. It was also evident from the greatly magnified TEM micrographs of the twice and four times crushed specimens displayed in Figure 3 that there were extinction contours at the grain boundaries and that the grain boundaries were not well defined. The viability of ultrafine-grain AA5083 low-temperature superplasticity was investigated in this work. As a structural material, the conventional non-heat-treatable Al–Mg-based alloy AA5083 exhibits intriguing properties. Because of the slightly divergent trend, precipitation or the recrystallization of the Equal Channel Angular Pressing (ECAP) process is assumed to be to blame, and as a result, the quantity of energy released affects the specific heat capacity.

Microstructural Change by Static Annealing

An ECAP method was used to examine the thermal stability of ultrafine-grained AA5083. Static heat treatment was applied to one and two pressed specimens, which were annealed at 548 K for one hour. In the case of the two-times-pressed specimens, the grain boundary was quite evident following the annealing process, with the exception of the as Equal Channel Angular Pressing (ECAPed) pressed specimen shown in Figure 4(a). The grains were approximately 0.5 μm in size, indicating minimal grain development, as shown in Figure 4(b).

In the two pressing specimens, there are some recrystallized grains with a grain size of about 5 μm, Figure 5(a) and (b). As depicted in Figure 5, prior observations acknowledged that the lattices near grain boundaries experienced significant distortion. Additionally, in strongly plastically deformed metallic materials, grain boundaries with indistinct features exhibited multiple facets and either regular or irregular step alignments [47, 48]. The grain border energy was significantly increased owing to the presence of extrinsic dislocations, which had a density of approximately 1018 m^{-2} in the grain boundaries. Even at comparatively low temperatures, grains with non-equilibrium grain borders may exhibit grain development [6, 49]. According to Hasegawa et al. [52], twice ECAPed pressing revealed

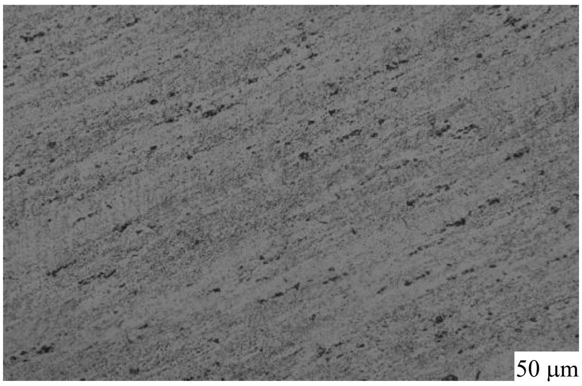

Figure 3. AA5083 has received, as measured by optical microstructure [19].

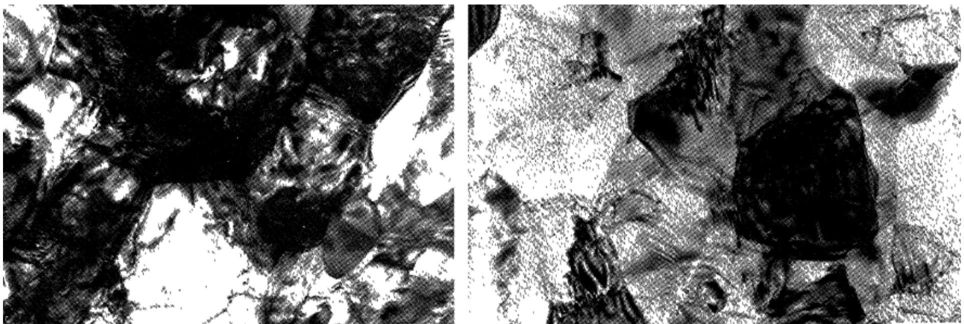

Figure 4. (a) to (b) TEM micrographs of pressed AA5083 with one and two pressings that have been greatly enlarged [14].

the presence of a duplex structure with parts of both huge and sub-micrometer grains. A duplex structure containing both large and sub-micrometer grain sections was observed by twice ECAPed pressing, as reported by Hasegawa et al. [52].

Microstructural Change at SAED Pattern

An optical image taken prior to the ECAP procedure (Figure 5) depicts the 210-μm grains aligned in the directions of tensile loading. Subgrain bands parallel to the shear surface form in the case of a single pass, as depicted in Figure 6(a), with a grain size of 210 nm in width and 710 nm in length. In two passes, the subgrain bands vanish (Figure 6(b)), and an equiaxed grain with a diameter of approximately 510 nm emerges. Compared with a single ECAP pass, the diffraction pattern generates a ring pattern in the SAED pattern. This demonstrates that high-angle misorientation is caused by the angles formed between the grain boundaries in polycrystals. This implies that the greater plastic deformation of the subgrains created in two passes, as opposed to the subgrains formed in one pass, has exacerbated the misorientation of the grains. As the number of passes increases, the subgrains at the low-angle grain border shift to the high-angle grain boundary. The grain size was lowered to as little as 160 nm in the four and eight-pass cases depicted in Figure 6(c) and (d), yielding grains that were closer to equiaxed than in the two-pass instance.

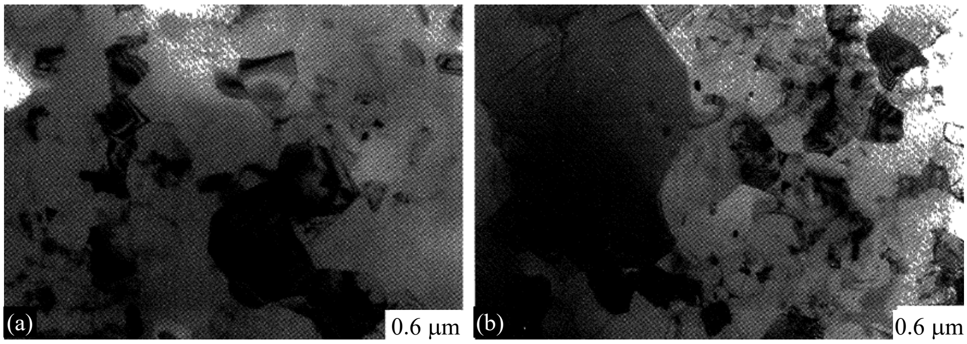

Figure 5. (a) to (b) TEM micrographs of ECAPed pressed AA5083 after one and two pressings, annealed at 548 K for 1.2 hours [29].

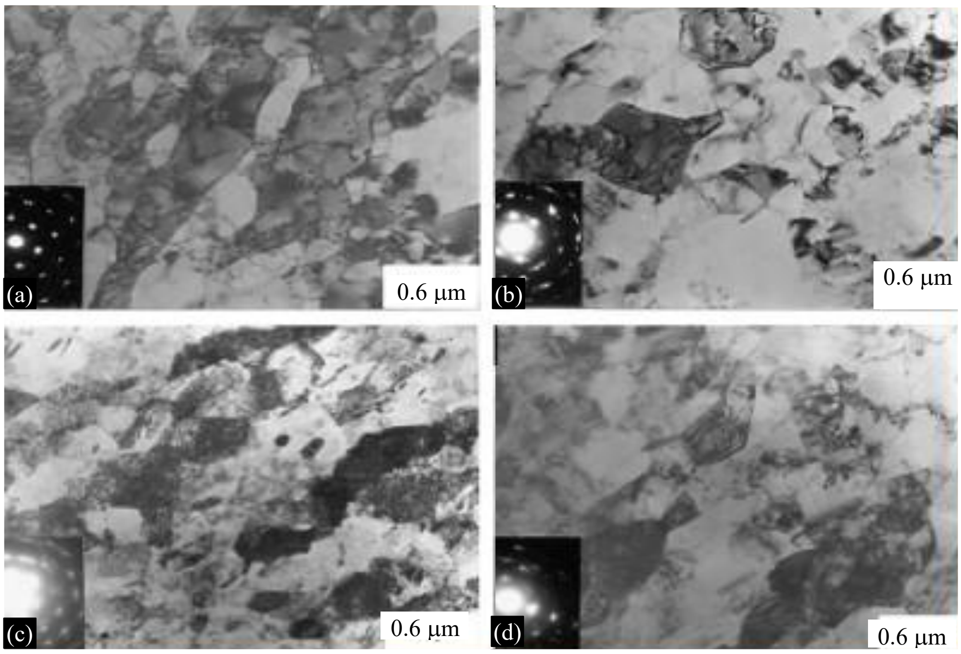

Figure 6. (a–d) TEM micrographs and corresponding SAED patterns were used to analyze the 5083 Al alloy, subjected to pressing at 90° in route B_c. The alloy underwent one and two passes for examination [39].

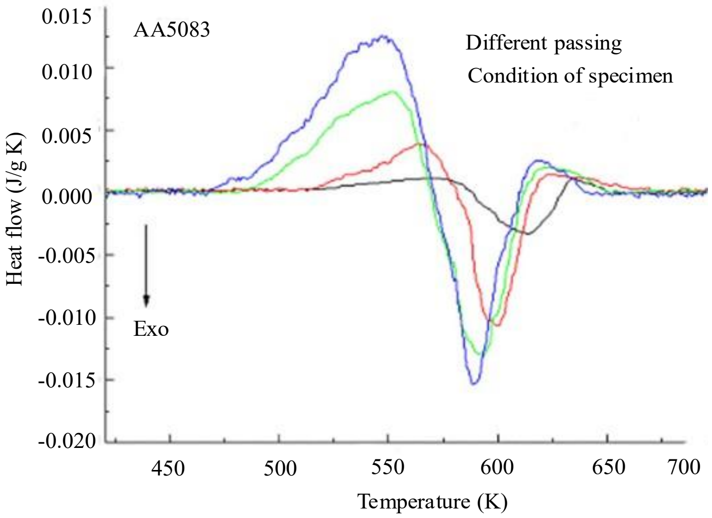

Figure 7. Heat flow of ECAPed AA5083 [51].

As the number of passes increases, a high-angle grain boundary is formed, as evidenced by the SAED patterns in one and two passes shown in Figure 7, which display more vibrant ring patterns than the two-pass patterns. However, when the material undergoes substantial plastic deformation, the lattice surrounding the boundaries becomes severely distorted, which is why the grain boundaries of single pass and double passes are indefinite as opposed to those of single pass and double passes. Moreover, owing to the threefold increase in grain boundary energy, these grain boundaries exhibit extrinsic grain boundary dislocations at approximately 1018 m^{-2} [60, 61]. It has been established that grain growth occurs, even at relatively low temperatures, at the non-equilibrium grain boundaries characterized by elevated internal energy and long-range stress.

Mechanical Properties of Materials

At Room Temperature

Figure 8 illustrates how the microhardness of ECAP-pressed AA5083 varies with the number of presses. The microhardness shows a significant shift as a result of applying more pressure. This is similar to the finding published by Iwahashi et al. [55], which showed that after just one pressing, pure Al microhardness significantly increased from 20 to 38 HV [56]. Nevertheless, the microhardness exhibited a negligible increase following two and three consecutive pressings before reaching saturation beyond three repetitions. The formation of subgrain bands and heightened dislocation density arising from shear deformation within the initial grain interior are responsible for work hardening. This leads to a substantial increase in microhardness following a single pressing. In contrast, it is hypothesized that the dynamic recovery brought about by subgrain rotation and dislocation rearrangement that forms the grain boundary during recurrent pressing is the cause of the microhardness constant value with the number of pressings [52]. Figure 9 shows how the elongation, yield strength, and tensile strength change as the number of pressings increases. The tensile strength of pre-material AA5083 developed steadily; however, after one pressing, the yield strength increased to 252 MPa, and after two pressings, it reached 293 MPa. The number of pressings did not affect the elongation. Figure 8 displays typical real stress–strain curves derived for ECAP-pressed Al alloys [57–60].

While the ECAP-pressed one showed a modest amount of strain hardening, the pre-material AA5083 exhibited the typical strain hardening behavior. Recent research indicates that this is highly associated with both the number of dislocations required to deform the ultra-thin grains and the annihilation kinetics of extrinsic GB dislocations induced by extreme plastic deformation [10, 53, 54]. There was a slight variation from the typical behavior of ultrafine-grained materials, although. According to previously published research, ultrafine-grained materials do not show any signs of strain hardening [5, 6, 19]. However, the cause was not clear in this study. This will be investigated in future research. In contrast, the number of pressings did not affect the strain hardening behavior.

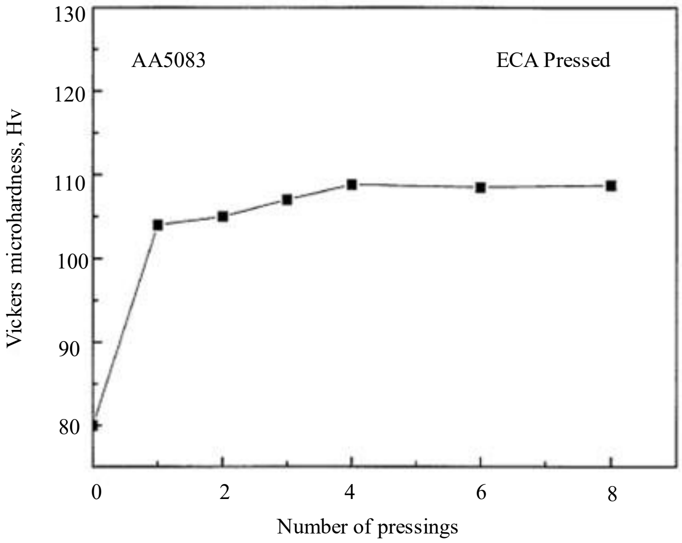

Figure 8. Vickers hardness in relation to the quantity of ECAP-pressed AA5083 presses [57].

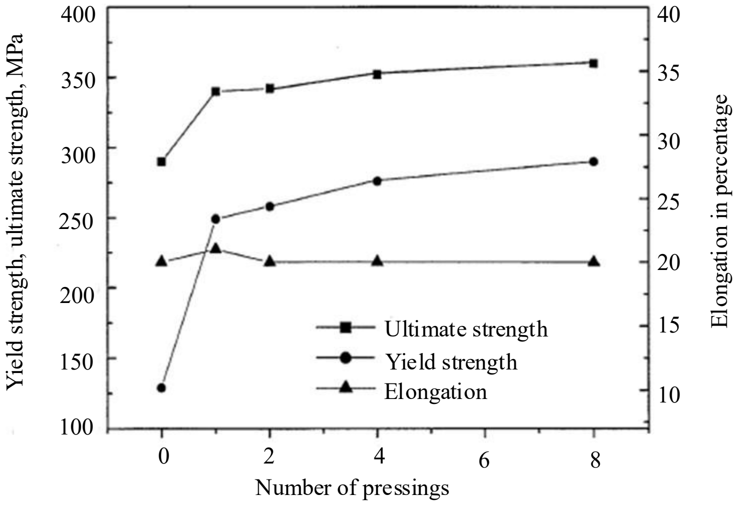

Figure 9. Tensile properties of ECAP-pressed AA5083 are affected by the quantity of pressings [40].

In Figure 9, the yield strength, ultimate strength, and elongation of ECAP-pressed AA5083 are compared with those of AA5083-O and the strongest form of AA5083 that is currently available [55]. ECAP-pressed AA5083 has a yield strength that is over double the amount compared to the AA5083-O material and a tensile strength that is around 63 MPa higher. In addition, compared with the AA5083-H321 material, the ECAP-pressed AA5083 material showed a notable increase of approximately 18% in yield strength and ultimate strength while maintaining the same elongation. The behavior of typical materials is noticeably different from this discovery of increased strength with no commensurate decrease in elongation. This result demonstrates that the refining of the grain by the ECAP process is responsible for the improvement in the mechanical properties.

At 548 K

It is commonly recognized that improved superplasticity is introduced by smaller grain sizes. This is because superplastic deformation primarily involves grain boundary sliding (GBS). Superplasticity is generally observed in metallic materials with grain sizes smaller than 12 μm at strain rates between 10^{-5} and 10^{-3} s^{-1} and at temperatures exceeding 0.8 Tm. Furthermore, it is well known that the ideal circumstances for superplasticity are low strain, less than 10^{-3} s^{-1}, and high temperature. These two factors pose significant challenges to the practical application of superplasticity. Therefore, research using ultrafine grains has been actively conducted to achieve superplasticity at low temperatures and high strain rates [56, 57]. The ultrafine-grained AA5083 was subjected to tensile tests at 548 K (0.58 Tm) with an initial strain rate of 1.06×10^{-4} s^{-1} to investigate low-temperature superplasticity. Figure 10 shows the pre-material AA5083 curve and the stress–strain curves.

The flow stress of the as received AA5083 was approximately 75 MPa, whereas the flow stresses of AA5083 that were pressed once and twice were 63 and 55 MPa, respectively. Following one and two pressings, the elongations were 170% and 230%, respectively. This is a significant increase over the AA5083 as received. This is also consistent with the finding of Berbon et al. [6], which showed that the elongation of the repeatedly ECAP-pressed one rose dramatically at a greater strain rate in the Al-5.5 Mg-2.2Li-0.12Zr alloy. The grip (a) and deformed (b) sections of the OM microstructures for the twice-pressed AA5083 subjected to tensile deformation are shown in Figure 11. In the grip section, the grain grew from its original size of 0.4 μm to approximately 10 μm, and no holes were observed. Grain elongation occurred parallel to the tensile direction; however, local grain growth occurred in the distorted region [57]. Additionally, the distorted section contained numerous cavities. This is implied by the fact that cavities typically occur along grain boundaries parallel to the direction of tensile stress, indicating that stress concentration caused by GBS may be the cause of the cavities. Nonetheless, the decline in flow stress and increase in elongation can be attributed to the high-angle grain boundaries produced by the repeated ECAP [58]. These limits may slip readily, which could be a major factor in the low-temperature superplasticity that results. It is generally anticipated that materials with extremely fine grains (less than 1.2 μm) will exhibit superplasticity at temperatures lower than 598 K and strain rates greater than 10^{-4} s^{-1}. As shown in Table 2, commercial AA5083 did not produce adequate results for low-temperature superplasticity [59]. Grain diameters larger than 12 μm in alloys in the Al–Mg binary system do not significantly elongate at relatively mild temperatures and strain rates [39, 40]. A grain size of roughly 0.3 μm was produced by Wang et al. [35] after applying the ECAP to the Al-3Mg alloy. Additionally, Kawazoe et al. [36] created an ultrafine-grained Al-4.8Mg alloy with a 0.4 μm grain size using the ECAP. Nevertheless, in both cases the elongation did not exceed 210%, indicating that low-temperature superplasticity was not achieved. It is possible that other elements, such as Sc [58,59], Mn [40, 41], or Zr [40], were added to improve superplasticity at high temperatures. However, the features of low-temperature superplasticity were fundamentally below 210% [42]. For the Al-4.45Mg-0.5Mn alloy, accumulative roll bonding produced a small grain size of 0.28 μm, which resulted in a notable elongation of 230% at 498 K and 1.2×10^{-3} s^{-1} [43]. The aforementioned findings imply that

Table 2. Tensile characteristics of commercial AA5053 and ECAP-pressed AA5083.

	UTS (MPa)	YS (MPa)	EI (%)
ECAP AA5083 (two passes)	352	276	20
AA5083-O	290	145	22
AA5083-H321	315	230	16

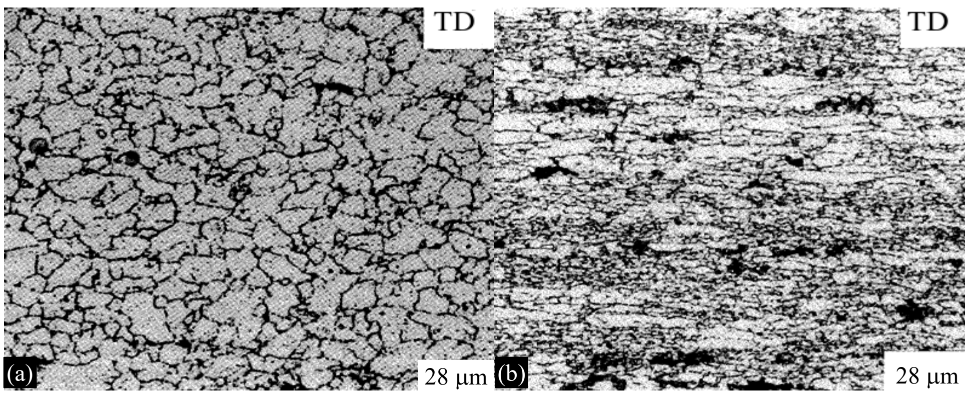

Figure 10. (a) to (b) Optical Microscopy (OM) the grip section (a) and the distorted region (b) are micrographed after eight times that ECAP-pressed AA5083 29].

attaining a high-angled grain boundary is a successful means of achieving low-temperature superplasticity in commercial AA5083.

Analysis of Thermal Effect

The Differential Scanning Calorimetry (DSC) analysis results for the temperature range of 323–855 K at a heating rate of 12 K/min are shown in Figure 12. One exothermic peak and two endothermic peaks are observed. Table 3 lists the measurements of the heat of transition, peak temperature, and start. The ECAP process significantly affects the start temperature and heat of transition, whereas the number of passes and peak temperature remain unchanged for one exothermic peak and two endothermic peaks. Grains are thought to be formed via endothermic and exothermic reactions resulting from crystallization and recrystallization, which is accomplished by the ECAP process [12].

We investigated a temperature range of 445–665 K. Numerous endothermic and exothermic DSC peaks were observed in this temperature range [13]. We observed the formation of the first endothermic DSC peak and a combination of endothermic and exothermic features for the second peak, which resulted from dissolution and transition. Dissolution was indicated by the third endothermic peak. We believe that when the heat of fusion reaches ECAP, the transition temperature decreases to that value. At temperatures ranging from 548 to 748 K, AA5083 can recover and recrystallize [14]. The Al6Mn precipitate appeared under heat treatment conditions, as shown in Figure 13. Thus, precipitation of Al_3Mg, Al6Mn, etc., had an impact on this temperature range of AA5083. Utilizing TEM and X-ray Diffraction. Every peak in eight passes has been examined. First, examining the XRD pattern in Figure 14, we can see that the precipitation peak of Al6Mn is located at 548, 548, and 675 K. The specimen showed no evidence of this peak after eight as ECAPed passes. This shows that the endothermic first peak is where the Al6Mn phase precipitates. The TEM image of the specimen was water-quenched at 548 K in the first endothermic peak interval. Compared to the grain boundaries in Figure 11(a), which are less defined, Figure 11(b) depicts grains that have been unpolished to a size of up to 210 nm. This is the outcome of the thermal effect, lowering the dislocation, which lowers the boundary energy. The precipitate, measuring 32 nm in diameter and 110 nm in length, is depicted in Figure 11(b), together with the results of the Energy Dispersive X-ray Spectroscopy (EDS). Analysis, which indicates a 6:1 Al:Mn ratio. As further supported by the results of earlier investigations [60]. Because of recovery and recrystallization, the microhardness rapidly decreased in the 498–548 K temperature range. Four passes of the ECAPed sample showed an endothermic peak at 510 K, which we believe is caused by recrystallization and recovery. The specimen that underwent eight ECAP passes produced its initial endothermic peak as a result of repeated precipitation and recovery reactions. More precipitates are visible in Figure 11(b), when compared to the image of the grain, which has expanded to a size of 510 nm. This demonstrates that precipitation can occur as low as 598 K, or within the exothermic peak range. With an increasing number of passes, the opening temperature of the exothermic peak decreases from 623 to 568 K. The strain energy that the material accumulated as the number of passes increased was directly impacted by this. The dislocation produced during strong plastic deformation raises the strain energy, as expressed by the following formula [61]:

$$E_{stored} = Gb^2 \frac{\rho}{4\pi k} ln\left(b\sqrt{\rho}\right) \quad (2)$$

Where, ρ is the dislocation density, μ is Poisson's ratio, κ is the arithmetic average of (v) and (1–v), G is the shear modulus and b is the Burgers vector. Equation (2) is governed by.

The endothermic and exothermic peaks of the ECAPed commercial 5083 Al alloy shift towards lower temperatures with an increase in the number of processing steps. This is because the driving power required for nucleation increases while the amount of dislocation created during deformation increases, which lowers the temperatures of recovery and recrystallization. Thermal instability is the main issue when using the ECAP technique to treat materials. More dislocations are generated by deformation, which lowers the thermal stability of the material and results in recrystallization at low temperatures. The results of a previous investigation were supplemented with Sc and Zr to overcome this thermal

ISSN: 2230-9845 (Online), ISSN: 2321-516X (Print)

instability and produce small precipitate particles. Al_3Sc and Al_3Zr precipitates with a nanoscale are generated when Sc and Zr are mixed with an aluminum matrix phase. These precipitates have a coherent or semi-coherent interaction with the Al matrix and exhibit exceptional high-temperature safety. Additionally, the Al_3Sc and Al_3Zr precipitates are dispersed throughout the grains, preventing grain expansion and structural coarsening by impeding grain boundary movement at elevated temperatures [48, 49].

Table 3. The 5083 Al alloys' temperature and heat of fusion were determined using ECAP.

DSC scan	Number of ECAP	Single pass	Double passes
First endothermic	Onset temperature (K)	513.5	511.8
	Peak temperature (K)	567.7	564.3
	Heat of transition (J/g)	0.22	0.46
Second endothermic	Onset temperature (K)	598.8	578.3
	Peak temperature (K)	613.1	601.7
	Heat of transition (J/g)	-0.09	-0.30
Third endothermic	Onset temperature (K)	609.4	602.7
	Peak temperature (K)	633.4	625.6
	Heat of transition (J/g)	0.03	0.11

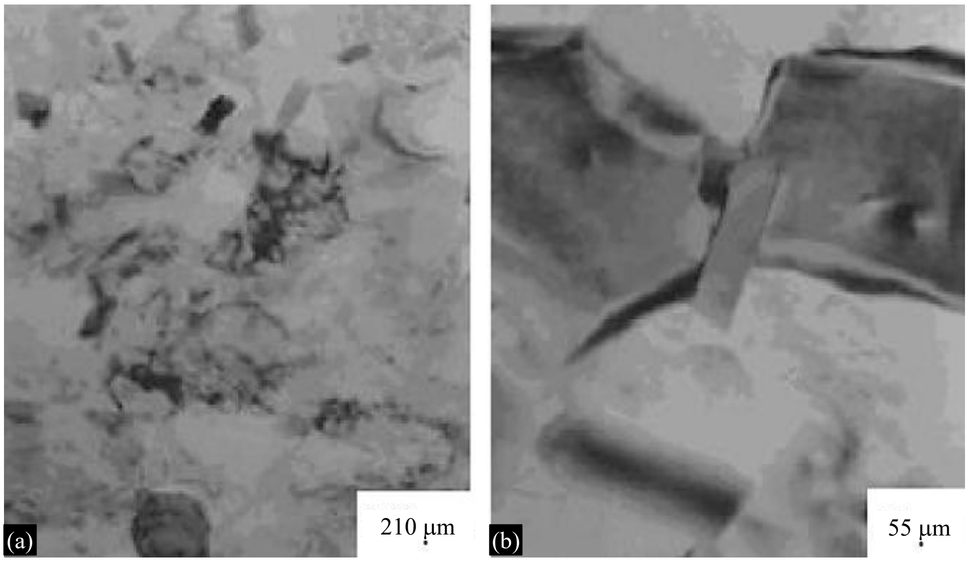

Figure 11. (a) to (b) Microstructure of alloys 5083 Al treated at 548 K with ECAP [33].

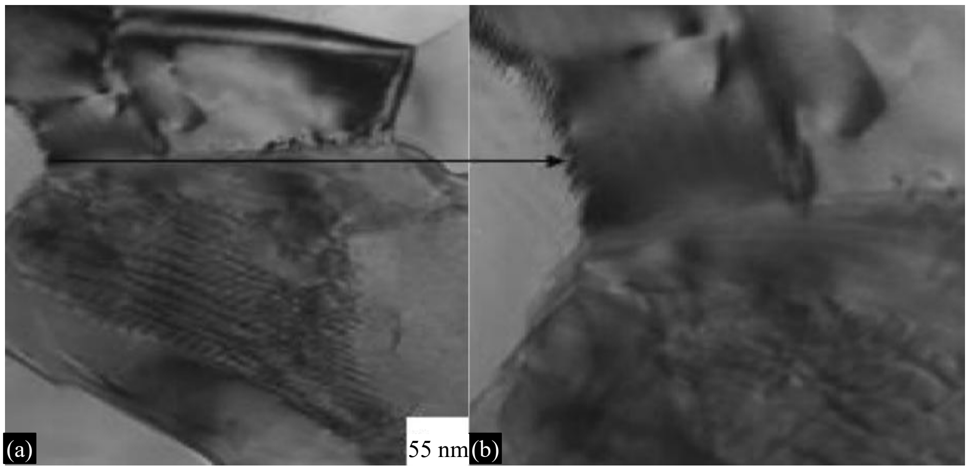

Figure 12. (a) to (b) The expanded fringes and moiré are visible in the microstructure of the 5083 Al alloys that have undergone ECAPing at 548 K [41].

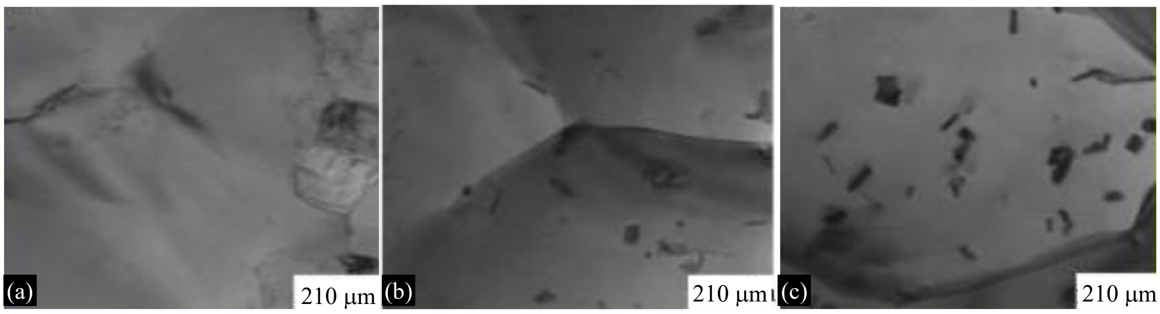

Figure 13. (a–c) Microstructure of alloys 5083 Al treated at 598 K with ECAP [57].

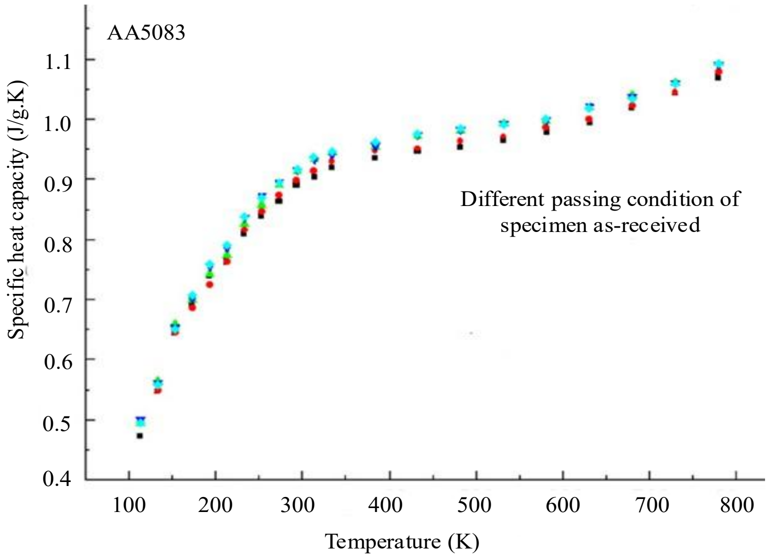

Figure 14. ECAP-fabricated 5083 Al alloys have a specific heat capacity ranging from 125 to 825 K [30].

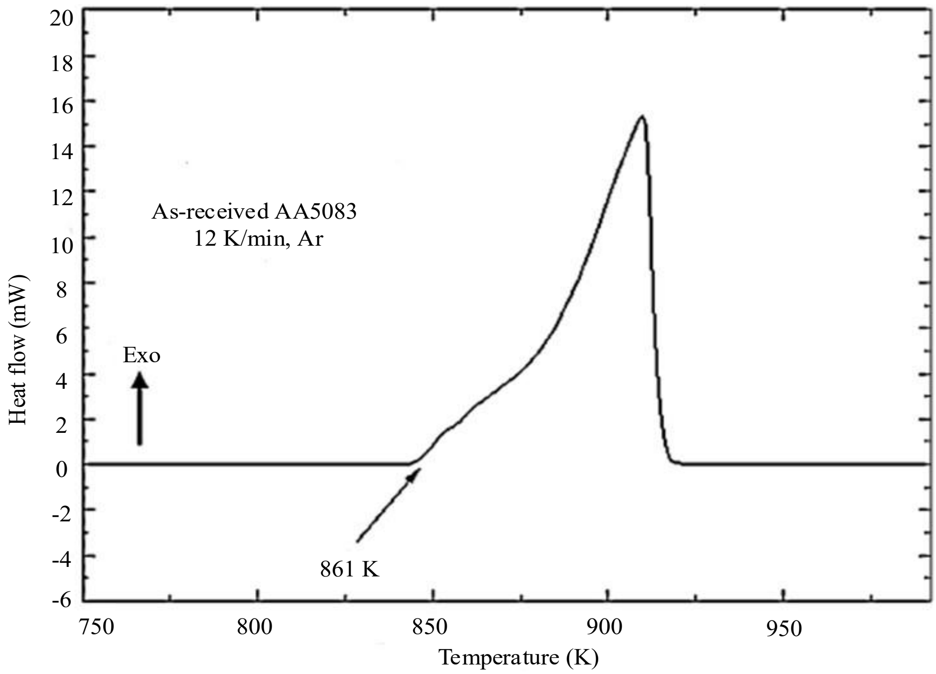

Figure 15. The 5083 Al alloy as received, with its differential scanning calorimetry curve indicating the partial melting that occurred at 862 K [60].

As illustrated in Figure 15, the specific heat capacity was computed at temperatures ranging from 125 to 825 K. For each sample, the specific heat capacity increased in a temperature-dependent manner. At <325 K, the specific heat capacity is not affected by ECAP; nevertheless, in the high-temperature region, it increases as ECAP passes. These differences are related to the energy state shown in Figure 15. Crystallization and recrystallization brought on by the ECAP process over 575 K were determined [49]. When Zr or Sc is not added, grain development occurs even at 525 K, but when Sc is added, the grain size remains extremely small until 625 K. This outcome is amply demonstrated by the DSC melting point measurement of AA5083. The melting temperature of AA5083 in the absence of Sc is shown in Figure 14 and is approximately 35 K lower than that at 900 K [18] reported by Park. This suggests that one of the elements contributing to the thermal stability of the Al–Mg type is either Sc or Zr.

CONCLUSIONS

Using this approach, ECAP of commercial AA5083 was accomplished effectively at 498 K using route B_c. The microstructure exhibited homogeneity, characterized by parallel bands of an elongated substructure with an average length of 0.9 µm and a width of 0.3 µm. An equiaxed extremely fine-grained structure with a 0.4-µm grain size was obtained after two pressings. After 1.2 h of annealing at 548 K, the extremely tiny grains obtained from a single pressing were thermally stable; however, AA5083 after two pressings displayed uneven grain growth. After one pressing, the yield strength of the as received AA5083 significantly increased to 252 MPa, and after two pressings, it reached 293 MPa. Conversely, the elongation remained relatively constant, while the number of pressings led to a progressive increase in the tensile strength. With an increased number of pressings, ECAP AA5083 with a 0.4-µm grain size showed an increase in elongation and a decrease in flow stress at 548 K. It also demonstrated behavior akin to that of superplastic materials, with an elongation to failure exceeding 210%. In this work, the effects of grain atomization on the characteristics of ECAPed AA5083 were observed through thermal and structural analyses. The second exothermic peak, which was generated in proportion to the number of ECAP passes, was created by the precipitation of Al6Mn. Additional evidence of precipitation was observed in the second exothermic peak.

Conflict of Interest Statement

The authors declare that they have no known competing financial interests or personal relationships that could have influenced the work reported in this paper.

REFERENCES

1. Valiev RZ, Islamgaliev RK, Alexandrov IV. Bulk nanostructured materials from severe plastic deformation. Prog Mater Sci. 2000;45:103–189. doi:10.1016/S0079-6425(99)00007-9.
2. Segal VM, Reznikov VI, Drobyshevskiy AE, Kopylov VI. Plastic working of metals by simple shear. Russ Metall. 1981;(1):99–105.
3. Segal VM. Materials processing by simple shear. Mater Sci Eng A. 1995;197(2):157–164. doi:10.1016/0921-5093(95)09705-8.
4. Valiev RZ, Ivanisenko YV, Rauch EF, Baudelet B. Structure and deformation behaviour of Armco iron subjected to severe plastic deformation. Acta Mater. 1996;44:4705–4712. doi:10.1016/S1359-6454(96)00156-5.
5. Zhao S, Yin S, Liang X, Cao F, Yu Q, Zhang R, et al. Deformation and failure of the CrCoNi medium-entropy alloy subjected to extreme shock loading. Sci Adv. 2023;9(18):eadf8602. doi:10.1126/sciadv.adf8602.
6. Berbon PB, Langdon TG, Tsenev NK, Valiev RZ, Furukawa M, Horita Z, et al. Fabrication of bulk ultrafine-grained materials through intense plastic straining. Metall Mater Trans A. 1998;29:2237–2243. doi:10.1007/s11661-998-0101-6.
7. Iwahashi Y, Furukawa M, Horita Z, Nemoto M, Langdon TG. Microstructural characteristics of ultrafine-grained aluminum produced using equal-channel angular pressing. Metall Mater Trans A. 1998;29:2245–2252. doi:10.1007/s11661-998-0102-5.

8. Valiev RZ, Islamgaliev RK, Kuzmina NF, Li Y, Langdon TG. Strengthening and grain refinement in an Al-6061 metal matrix composite through intense plastic straining. Scr Mater. 1998;40:117–122. doi:10.1016/S1359-6462(98)00398-4.
9. Valiev RZ, Kozlov EV, Ivanov YF, Lian J, Nazarov AA, Baudelet B. Deformation behaviour of ultra-fine-grained copper. Acta Metall Mater. 1994;42(7):2467–2475.
10. Ferrasse S, Hartwig KT, Goforth RE, Segal VM. Microstructure and properties of copper and aluminum alloy 3003 heavily worked by equal channel angular extrusion. Metall Mater Trans A. 1997;28:1047–1057. doi:10.1007/s11661-997-0234-z.
11. Singh N, Agrawal MK, Saxena KK, Kumar S, Prakash C. Advancement and influence of designing of ECAP on deformation and microstructure properties of the AA5083 under thermal effects. Int J Interact Des Manuf. 2024;18:1809–1827. doi:10.1007/s12008-023-01213-y.
12. Valiev RZ, Alexandrov IV. Nanostructured materials from severe plastic deformation. Nanostruct Mater. 1999;12(1–4):35–40. doi:10.1016/S0965-9773(99)00061-6.
13. Alexandrov IV, Valiev RZ. Nanostructures from severe plastic deformation and mechanisms of large-strain work hardening. Nanostruct Mater. 1999;12(5–8):709–712. doi:10.1016/S0965-9773(99)00223-8.
14. Shin DH, Kim WJ, Choo WY. Grain refinement of a commercial 0.15% C steel by equal-channel angular pressing. Scr Mater. 1999;41(3):259–262. doi:10.1016/S1359-6462(99)00156-6.
15. Shin DH, Seo CW, Kim J, Park KT, Choo WY. Microstructures and mechanical properties of equal-channel angular pressed low carbon steel. Scr Mater. 2000;42(7):695–699. doi:10.1016/S1359-6462(99)00422-4.
16. Shin DH, Kim BC, Kim YS, Park KT. Microstructural evolution in a commercial low carbon steel by equal channel angular pressing. Acta Mater. 2000;48(9):2247–2255. doi:10.1016/S1359-6454(00)00028-8.
17. Shin DH, Kim BC, Park KT, Choo WY. Microstructural changes in equal channel angular pressed low carbon steel by static annealing. Acta Mater. 2000;48(12):3245–3252. doi:10.1016/S1359-6454(00)00090-2.
18. Park KT, Kim YS, Lee JG, Shin DH. Thermal stability and mechanical properties of ultrafine grained low carbon steel. Mater Sci Eng A. 2000;293(1–2):165–172. doi:10.1016/S0921-5093(00)01220-X.
19. Semiatin SL, DeLo DP, Segal VM, Goforth RE, Frey ND. Workability of commercial-purity titanium and 4340 steel during equal channel angular extrusion. Metall Mater Trans A. 1999;30:1425–1435. doi:10.1007/s11661-999-0290-7.
20. Singh N, Agrawal MK, Verma SK, Tiwari AK. A review on effect of stress and strain distribution on AA5083 with respect to different channel angle of ECAP. Int Res J Adv Sci Hub. 2022;4(3):57–66. doi:10.47392/irjash.2022.013.
21. Semiatin SL, DeLo DP. Equal channel angular extrusion of difficult-to-work alloys. Mater Des. 2000;21(4):311–322. doi:10.1016/S0261-3069(99)00085-0.
22. Gao P, Ma Z, Gu J, Ni S, Suo T, Li Y, et al. Exceptional high-strain-rate tensile mechanical properties in a CrCoNi medium-entropy alloy. Sci China Mater. 2022;65:811–819. doi:10.1007/s40843-021-1798-6.
23. Japan Institute of Light Metals. Microstructure and properties of aluminum alloys. Tokyo: Japan Institute of Light Metals; 1991. p. 256–277.
24. Zhang T, Guo W, Su Z, Cao B, Sun X, Ren R, et al. Investigation of magnetic field arrangement on launching performance of multistage synchronous induction coilgun. IEEE Trans Plasma Sci. 2017;45(7):1436–1442. doi:10.1109/TPS.2017.2705639.
25. Djavanroodi F. Equal channel angular pressing of multi size copper wire. US Patent 10,773,286; 2020.
26. Pu HP, Liu FC, Huang JC. Characterization and analysis of low-temperature superplasticity in 8090 Al-Li alloys. Metall Mater Trans A. 1995;26:1153–1166. doi:10.1007/BF02670612.
27. Tian Y, Chen F. Short-range order-dependent dislocation mobilities in CrCoNi medium entropy alloy: Atomistic simulations and modeling. Int J Plast. 2024;172:103859. doi:10.1016/j.ijplas.2023.103859.

28. Shin DH, Joo YJ, Lee CS, Park KT. Grain elongation in a superplastic 7075 Al alloy. Scr Mater. 1999;41:269–274. doi:10.1016/S1359-6462(99)00160-8.
29. Shin DH, Joo YJ, Lee CS, Park KT. Grain elongation in a superplastic 7075 Al alloy. Scr Mater. 1999;41(3):269–274. doi:10.1016/S1359-6462(99)00160-8.
30. Shin DH, Lee CS, Kim WJ. Superplasticity of fine-grained 7475 Al alloy and a proposed new deformation mechanism. Acta Mater. 1997;45(12):5195–5202. doi:10.1016/S1359-6454(97)00185-7.
31. Singh N, Agrawal MK, Verma SK, Tiwari AK. Study of the effect of ECAPed method on the mechanical properties of AA 5083: An overview. Int Res J Adv Sci Hub. 2022;4(6):186–191. doi:10.47392/irjash.2022.044.
32. Chang SY, Lee JG, Park KT, Shin DH. Microstructures and mechanical properties of equal channel angular pressed 5083 Al alloy. Mater Trans. 2001;42(6):1074–1080. doi:10.2320/matertrans.42.1074.
33. Humphries CW, Ridley N. Cavitation during the superplastic deformation of an α/β brass. J Mater Sci. 1978;13:2477–2482. doi:10.1007/BF00808064.
34. Furukawa M, Horita Z, Nemoto M, Valiev RZ, Langdon TG. Microstructural characteristics of an ultrafine grain metal processed with equal-channel angular pressing. Mater Charact. 1996;37:277–283. doi:10.1016/S1044-5803(96)00131-3.
35. Furukawa M, Horita Z, Nemoto M, Valiev RZ, Langdon TG. Microstructural characteristics of an ultrafine grain metal processed with equal-channel angular pressing. Mater Charact. 1996;37(5):277–283. doi:10.1016/S1044-5803(96)00131-3.
36. Kawazoe M, Shibata T, Mukai T, Higashi K. Elevated temperature mechanical properties of A 5056 Al-Mg alloy processed by equal-channel-angular-extrusion. Scr Mater. 1997;36:699–705. doi:10.1016/S1359-6462(96)00446-0.
37. Kawazoe M, Shibata T, Mukai T, Higashi K. Elevated temperature mechanical properties of A 5056 Al–Mg alloy processed by equal-channel-angular-extrusion. Scr Mater. 1997;36(6):699–705. doi:10.1016/S1359-6462(96)00446-0.
38. Horita Z, Fujinami T, Nemoto M, Langdon TG. Equal-channel angular pressing of commercial aluminum alloys: Grain refinement, thermal stability and tensile properties. Metall Mater Trans A. 2000;31:691–701. doi:10.1007/s11661-000-0011-8.
39. Mao J, Kang SB, Park JO. Grain refinement, thermal stability and tensile properties of 2024 aluminum alloy after equal-channel angular pressing. J Mater Process Technol. 2005;159(3):314–320. doi:10.1016/j.jmatprotec.2004.05.020.
40. Woo SS, Kim YR, Shin DH, Kim WJ. Effects of Mg concentration on the quasi-superplasticity of coarse-grained Al–Mg alloys. Scr Mater. 1997;37(9):1351–1358. doi:10.1016/S1359-6462(97)00275-3.
41. Shuang S, Hu Y, Li X, Yuan F, Kang G, Gao H, et al. Tuning chemical short-range order for simultaneous strength and toughness enhancement in NiCoCr medium-entropy alloys. Int J Plast. 2024;177:103980. doi:10.1016/j.ijplas.2024.103980.
42. Singh N, Agrawal MK, Verma SK, Tiwari AK. RETRACTED: Impact design of die parameters on severe plastic deformation during equal channel angular pressing: An overview. E3S Web Conf. 2023;430:01255. doi:10.1051/e3sconf/202343001255. Retracted. doi:10.1051/e3sconf/202343000002.
43. Swaminathan K, Nandy A, Vasudevan R. Elevated temperature tensile flow and fracture behaviour of a recently developed Canadian Al-Mg-Mn alloy. J Mater Sci Lett. 1995;14:881–884. doi:10.1007/BF00639314.
44. Hsiao IC, Huang JC. Development of low temperature superplasticity in commercial 5083 Al–Mg alloys. Scr Mater. 1999;40(6):697–703. doi:10.1016/S1359-6462(98)00460-6.
45. Tsuji N, Shiotsuki K, Saito Y. Superplasticity of ultra-fine grained Al–Mg alloy produced by accumulative roll-bonding. Mater Trans JIM. 1999;40:765–771. doi:10.2320/matertrans1989.40.765.
46. Nakashima K, Horita Z, Nemoto M, Langdon TG. Influence of channel angle on the development of ultrafine grains in equal-channel angular pressing. Acta Mater. 1998;46(5):1589–1599. doi:10.1016/S1359-6454(97)00355-8.

47. Iwahashi Y, Wang J, Horita Z, Nemoto M, Langdon TG. Principle of equal-channel angular pressing for the processing of ultra-fine grained materials. Scr Mater. 1996;35(2):143–146. doi:10.1016/1359-6462(96)00107-8.
48. Tamm A, Aabloo A, Klintenberg M, Stocks M, Caro A. Atomic-scale properties of Ni-based FCC ternary and quaternary alloys. Acta Mater. 2015;99:307–312. doi:10.1016/j.actamat.2015.08.015.
49. Ding J, Yu Q, Asta M, Ritchie RO. Tunable stacking fault energies by tailoring local chemical order in CrCoNi medium-entropy alloys. Proc Natl Acad Sci U S A. 2018;115:8919–8924. doi:10.1073/pnas.1808660115.
50. Horita Z, Smith DJ, Furukawa M, Nemoto M, Valiev RZ, Langdon TG. An investigation of grain boundaries in submicrometer-grained Al-Mg solid solution alloys using high-resolution electron microscopy. J Mater Res. 1996;11:1880–1890. doi:10.1557/JMR.1996.0239.
51. Horita Z, Smith DJ, Nemoto M, Valiev RZ, Langdon TG. Observations of grain boundary structure in submicrometer-grained Cu and Ni using high-resolution electron microscopy. J Mater Res. 1998;13:446–450. doi:10.1557/JMR.1998.0057.
52. Nazarov AA, Romanov AE, Valiev RZ. On the nature of high internal stresses in ultrafine grained materials. Nanostruct Mater. 1994;4(1):93–101. doi:10.1016/0965-9773(94)90131-7.
53. Zhang XY, Liu Q, Wu XL, Zhu AW. Work softening and annealing hardening of deformed nanocrystalline nickel. Appl Phys Lett. 2008;93. doi:10.1063/1.3062849.
54. Japan Institute of Light Metals. Microstructure and Properties of Aluminum Alloys. Tokyo (Japan): The Japan Institute of Light Metals; 1991. p. 466.
55. Valiev RZ, Salimonenko DA, Tsenev NK, Berbon PB, Langdon TG. Observations of high strain rate superplasticity in commercial aluminum alloys with ultrafine grain sizes. Scr Mater. 1997;37:1945–1950. doi:10.1016/S1359-6462(97)00387-4.
56. Komura S, Berbon PB, Furukawa M, Horita Z, Nemoto M, Langdon TG. High strain rate superplasticity in an Al-Mg alloy containing scandium. Scr Mater. 1998;38:1851–1856. doi:10.1016/S1359-6462(98)00099-2.
57. Nieh TG. Subgrain formation and evolution during the deformation of an Al-Mg-Sc alloy at elevated temperatures. Scr Mater. 1997;36:1011–1016. doi:10.1016/S1359-6462(96)00479-4.
58. Horita Z, Furukawa M, Nemoto M, Barnes AJ, Langdon TG. Superplastic forming at high strain rates after severe plastic deformation. Acta Mater. 2000;48(14):3633–3640. doi:10.1016/S1359-6454(00)00182-8.
59. Singh N, Agrawal MK, Verma SK, Tiwari AK. A review on impact route process on AA5083 of back pressure through equal channel angular pressing. Mater Today Proc. 2023. doi:10.1016/j.matpr.2023.08.163.
60. Kim WJ, Wang JY. Microstructure of the post-ECAP aging processed 6061 Al alloys. Mater Sci Eng A. 2007;464:23–27. doi:10.1016/j.msea.2007.03.074.
61. Valiev RZ, Langdon TG. Principles of equal-channel angular pressing as a processing tool for grain refinement. Prog Mater Sci. 2006;51:881–981. doi:10.1016/j.pmatsci.2006.02.003.
62. Park KT, Kim YS, Lee JG, Shin DH. Thermal stability and mechanical properties of ultrafine grained low carbon steel. Mater Sci Eng A. 2000;293:165–172. doi:10.1016/S0921-5093(00)01220-X.

